Journal of Natural Gas Science and Engineering 49 (2018) 376–384

Contents lists available at ScienceDirect

Journal of Natural Gas Science and Engineering

journal homepage: www.elsevier.com/locate/jngse

# Incorporation of thermally labile additives in carbon membrane development for superior gas permeation performance

N. Sazali[a,b], W.N.W. Salleh[a,b,*], A.F. Ismail[a,b,**], N.A.H.M. Nordin[a,c], N.H. Ismail[a,b], M.A. Mohamed[d], F. Aziz[a,b], N. Yusof[a,b], J. Jaafar[a,b]

[a] Advanced Membrane Technology Research Centre (AMTEC), Universiti Teknologi Malaysia, 81310 Skudai, Johor Darul Takzim, Malaysia
[b] Faculty of Chemical and Energy Engineering (FCEE), Universiti Teknologi Malaysia, 81310 Skudai, Johor Darul Takzim, Malaysia
[c] Department of Chemical Engineering, Universiti Teknologi PETRONAS (UTP), 32610 Bandar Seri Iskandar, Perak, Malaysia
[d] Fuel Cell Institute (SELFUEL), Universiti Kebangsaan Malaysia, 43600 UKM Bangi, Selangor, Malaysia

ARTICLE INFO

*Keywords:*
Carbon membrane
Polyvinylpyrrolidone (PVP)
Microcrystalline cellulose (MCC)
Nanocrystalline cellulose (NCC)
Gas separation

ABSTRACT

Incorporating thermally labile polymer additives into carbon membrane development is highly practical due to its process simplicity and effective approach. In this study, different polymer composition of thermally labile additives such as polyvinylpyrrolidone (PVP), microcrystalline cellulose (MCC) and nanocrystalline cellulose (NCC) were introduced into the BTDA-TDI/MDI (P84-copolyimide) polymer solution. The P84-copolyimide based carbon tubular membranes were fabricated using dip-coating method and characterized in terms of its thermal stability, structural morphology and gas permeation properties. Initially, the NCC was introduced as a pore performing agent in the carbon membrane fabrication for carbon dioxide ($CO_2$) separation. Our finding indicated that the use of NCC as pore performing agent significantly promoted an increment of pore structure channel in carbon membrane. As a result, the high permeance as well as high selectivity was demonstrated in this study. Pure gas permeation tests were performed using $CO_2$, $CH_4$, $O_2$ and $N_2$ at room temperature. The increment of both gas permeance and selectivity were observed in the NCC-containing carbon membranes prepared with a composition of 7 wt%. The promising $CO_2/CH_4$ selectivity of 68.23 ± 3.27, $CO_2/N_2$ selectivity of 66.32 ± 2.18 and $O_2/N_2$ selectivity of 9.29 ± 2.54 with respect to neat carbon membrane were presented. Thus, upon further investigation, the potential of NCC as thermally labile additive in carbon membrane was assured.

## 1. Introduction

Challenges for polymeric membranes such as swelling and plasticization are no longer an issue for inorganic membranes. In general, inorganic membranes have great resistance to harsh environments and at high temperatures and pressures (Dalane et al., 2017). Among the inorganic membranes, carbon membranes, zeolite membranes and metallic membranes are the three candidates that have mostly been studied (Rungta et al., 2015). Indeed, the superior performance produced by carbon membrane can be achieved by a proper selection of membrane material which can withstand high thermal and mechanical stability (George et al., 2016). Carbon membrane is resulted from carbonization of polymeric precursors. As compared to polymeric membranes, the carbon membranes are immensely superior in terms of thermal and chemical resistance, thus results in no contamination, physical aging and plasticization as polymeric membrane (Adewole et al., 2013). In addition, the high pore volume of carbon membrane has provided higher selectivity and permeability as compared to polymeric membrane especially in the separation of similar gas molecules size such as $O_2/N_2$, $CO_2/CH_4$ and $CO_2/N_2$ (Hunt et al., 2010; Jones and Koros, 1994; Koresh and Soffer, 1986; Tanihara et al., 1999).

The developments of carbon membranes using polymer blend materials are among attractive strategies to improve their performances in term of permeability and selectivity. A variety of polymer blends has been explored in the recent years (Hosseini et al., 2014; Pirouzfar et al., 2014; Tiptipakorn et al., 2007; Yong et al., 2016). For instance, Itta and co-worker had successfully fabricated blending thermally stable polymer polyphenylene oxide (PPO) and thermally labile polymer poly vinylpyrrolidone (PVP) through a spin-coating technique (Itta et al., 2011). The best performance for hydrogen permeability obtained with PPO 15 PVP carbonized at 700 °C was 1121 Barrer (1 Barrer = $1 \times 10-10$ $cm^3$ (STP) $cm/cm^2$.s.cm Hg) and the values of

* Corresponding author. Advanced Membrane Technology Research Centre (AMTEC), Universiti Teknologi Malaysia, 81310 Skudai, Johor Darul Takzim, Malaysia.
** Corresponding author. Advanced Membrane Technology Research Centre (AMTEC), Universiti Teknologi Malaysia, 81310 Skudai, Johor Darul Takzim, Malaysia.
*E-mail addresses:* hayati@petroleum.utm.my (W.N.W. Salleh), afauzi@utm.my (A.F. Ismail).

https://doi.org/10.1016/j.jngse.2017.10.026
Received 4 July 2017; Received in revised form 30 August 2017; Accepted 20 October 2017
Available online 02 December 2017

selectivity for gas pairs such as $H_2/N_2$ and $H_2/CH_4$ were 163.9 and 160.9, respectively. The addition of thermally labile polyvinylpyrrolidone (PVP) created diffusion pathways and controlled selectivity for the carbon membranes derived from PPO 10 PVP and PPO 15 PVP. Moreover, carbon membrane carbonized at 550 °C from polyimide (PI) and polyvinylpyrrolidone (PVP) polymer blends exhibited an enhanced $O_2$ gas permeability from 560 to 810 Barrer and a reduced $O_2/N_2$ selectivity of $10^{-7}$ (Kim et al., 2005). Previous study has reported carbon membrane derived from PBI (poly-2,2′-(m-phenylene)-5,5′-bibenzimidazole) blends with PI (BTDA-TDI/MDI exhibited an open cell structure and a reduced thickness which led to a 50% higher pure water permeability and a larger pore diameter (Xing et al., 2013). Greater values of separation efficiency were achieved in higher than 90 wt% polyimide contents in these blends. In 2014, the carbon membranes fabricated from Kapton/PBI blends offered an incredible selectivity for majority of the gas pairs including $CO_2/CH_4$ (Pirouzfar et al., 2014).

By assuming the natural abundance of cellulose, bio inert behaviour, low weight and high strength and stiffness, the introduction of modification of this cellulose are needed for blending material applications. Recently, cellulose has been used in various application such nanocomposite material (Mohamed et al., 2015a, 2016a), membrane (Mohamed et al., 2015b), and bio-templated nanoreactor (Mohamed et al., 2016b, 2017c). Based on the author's knowledge, the study on microcrystalline cellulose (MCC) with PI has not yet been explored in the fabrication of carbon membrane. Rhim et al. have studied the thermophysical properties of carbon materials derived from MCC under vacuum and nitrogen atmospheres. The results indicated that both environment (vacuum and nitrogen) would increase the diffusivity and thermal conductivity of the material. Moreover, it is found that there are four regions corresponding to the stages of microstructural evolution during carbonization process (Rhim et al., 2010). Aside to MCC, the research on nanocrystalline cellulose (NCC) as one of the promising biodegradable material in the nanotechnology industry has been explored. Typically, NCC is obtained by acid hydrolysis of cellulose microfibrils by using sulphuric acid at a specific concentration for a desired amount time and temperature (Mohamed et al., 2017a, 2017b).

Based on literature, Bai et al. had prepared poly(vinylidene fluoride) (PVDF) composite membranes blended with (NCC) for ultrafiltration by a Loeb–Sourirajan (L–S) phase inversion process (Bai et al., 2012). The obtained membrane possessed an asymmetric structure which indicated the sponge-like dense layer and finger-like microporous supportive layer. They have proven that the mechanical property of resultant membrane was increased with addition of NCC, thus the degree of crystallinity was also increased to 52.1%. Another study has been done by Kaboorani et al. by adding NCC to polyvinyl acetate (PVA) at different loadings. This study showed that NCC could improve bonding strength of PVA in all conditions. In addition, thermal stability of PVA was significantly improved and structural studies revealed that variations in shear strength could be related to the quality of NCC dispersion in the PVA matrix (Kaboorani et al., 2012). The main interest of utilizing NCC in this study is due to their rod-like nanostructure and low decomposition temperature. The nanostructure of NCC would ease to be slit within polymer chain as compared to microstructure additive. Furthermore, NCC can be used as pore forming agent due to their premature decomposition would create channels to assist gas permeation.

The research on polymer blends has grown rapidly in the carbon membrane fabrication due to the formation of porous structure since the thermally labile polymer is completely decomposed at a lower temperature than the thermally stable polymer. As one of the interesting results on the addition of a thermally labile polymer, carbon membranes derived from the polymer blends showed a high permeability and selectivity even through microporous carbon membrane structures (Lee et al., 2007). Therefore, this study would focus on the development of carbon membrane by blending with three different thermally labile additives (NCC, MCC, and PVP) with polyimide particularly for $CO_2$ gas permeation. The results on the physicochemical properties and gas permeation performance of the resultant carbon membranes were compared and discussed.

## 2. Experimental section

### 2.1. Materials

Polyimide BTDA-TDI/MDI (P-84), polyvinylpyrolidone (PVP) and microcrystalline cellulose (MCC) were procured from Sigma Aldrich. N-methyl-2-pyrrolidone (NMP) was purchased from Merck (Germany). All chemicals were directly used without further purification. Nanocrystalline cellulose (NCC) was synthesized, in-house according to experimental procedure as reported in previous studies (Mohamed et al., 2015c). Porous tubular ceramic support ($TiO_2$) with 8 cm in length, 3 mm thickness and average pore size of 0.2 μm (porosity of 40–50%) was purchased from Shanghai Gongtao Ceramics Co. Ltd.

### 2.2. Carbon membrane preparation

Polymer solution consisting of 15% of P-84 (relative to total wt.) and NMP was prepared and stirred under constant stirring condition at 80 °C. A predetermined amount of additives (Table 1) were introduced into the solution and were continuously stirred to obtain homogenous solution. The solution was sonicated for 12 h in order to remove any trapped bubbles. The tubular support was then dip-coated for 45 min. Afterward, the resultant membranes were immersed in methanol for 2 h, followed by placing it inside the oven at 100 °C for 24 h in order to remove the solvent.

Carbon membranes were prepared by carbonization process of the supported polymeric membranes. For carbonization process, the supported polymeric membranes were heat treated in Carbolite horizontal tubular furnace at 800°C under nitrogen gas flow (200 ml/min). The detailed experimental procedures were conducted based on our previous studies (Sazali et al., 2017). Flat sheet carbon membranes (without substrate) were also prepared using similar procedure for characterization purposes.

### 2.3. Membrane characterization

Thermogravimetric analysis (TGA) was used to characterize thermal stability of polymeric membranes. TGA records the weight changes of the sample when the sample is heated up continuously. In this study, the sample was heated from room temperature to 900 °C at the heating rate of 10 °C $min^{-1}$ with nitrogen flow rate of 20 mL $min^{-1}$. Scanning electron microscopy was used to observe the membrane structure and morphology. Prior to the observation, the samples were coated with gold by employing a scanning electron microscope (TM3000, Hitachi) with a potential of 10 kV. Fourier Transform Infrared Spectroscopy (FTIR), Single Reflection Diamond for the Spectrum Two) (PerkinElmer, L1600107) was used to distinguish the actuality of the functional groups in a membrane. The presence of any element, compound or phase of the prepared carbon membranes were examined on X'Pert PRO X-ray different fractometer (XRD) from PANalytical with the diffraction angle from 2θ from 10° to 50°. Ni-filtered CuKα radiation

**Table 1**
Dope formulation for the preparation of carbon membrane.

| Sample | Composition (wt.%) | |
|---|---|---|
| | P-84 Polyimide | Additive |
| PI/NCC | 15 | 7 |
| PI/MCC | 15 | 7 |
| PI/PVP | 15 | 9 |

with a wavelength of λ = 1.54 Å was applied in the experiments. The interplanar distance (d-spacing) of the carbon membranes was calculated using Bragg equation.

### 2.4. Pure gas permeation measurements

The carbon tubular membranes were tested in gas permeation system as described in our previous study (Sazali et al., 2015a, 2015b). The carbon tubular membrane was placed inside a tubular stainless-steel module of 14 cm in length. To avoid any leakage on the module, the membrane was fitted with rubber O-rings. Pure gas $CH_4$ (0.380 nm), $N_2$ (0.364 nm), $O_2$ (0.346 nm) and $CO_2$ (0.330 nm) and were fed separately, in that order, into the module at a trans-membrane pressure of 8 bars. The permeance, $P/l$ (GPU) and selectivity, $\alpha$ of the membranes were calculated using equations as described in our previous studies (Sazali et al., 2017).

## 3. Results and discussion

### 3.1. Thermogravimetric analysis (TGA)

The thermogravimetric curves of NCC, PI, and PI/NCC were displayed in Fig. 1. On the account of differences in chemical constitution, all polymers were decomposed at different temperature. As shown in Fig. 1, NCC was stable up to 170 °C with a slight weight loss at around 100 to 150 °C due to evaporation of moisture content and other volatile components in the sample (Sun et al., 2016). It was observed that the NCC underwent thermal degradation (from 200 to 400 °C) earlier than the other membrane samples due to the decomposition of sulphate groups. The presence of sulphate groups which were introduced onto the NCC particles during hydrolysis process might also affect the thermal stability of NCC due to the dehydration reaction involving the sulphate groups (Rubentheren et al., 2016). PI-copolyimide curve shows a single-step weight loss from 530 to 630 °C indicated an excellent thermal stability of polymer with decomposition temperature at 535.5 °C. The approximately 4% weight loss of the pure PI at 100 °C was due to the evaporation of moisture in the sample. Two stages of weight loss were observed in the PI/NCC curve. The first weight loss around 280–375 °C was related to the thermal decomposition of NCC while the second decomposition from 375 to 565 °C was attributed to the thermal decomposition of PI.

The TGA profiles for MCC, PI, and PI/MCC are graphically presented in Fig. 2. Analysis of TGA curve for MCC showed that the MCC was stable up to 337 °C. The weight loss of MCC between 291 °C and 337 °C was attributed to the decomposition of micro cellulose particles and the evolution of non-combustible gases such as carbon dioxide, carbon monoxide, formic acid and acetic acid (Das et al., 2010). Similar

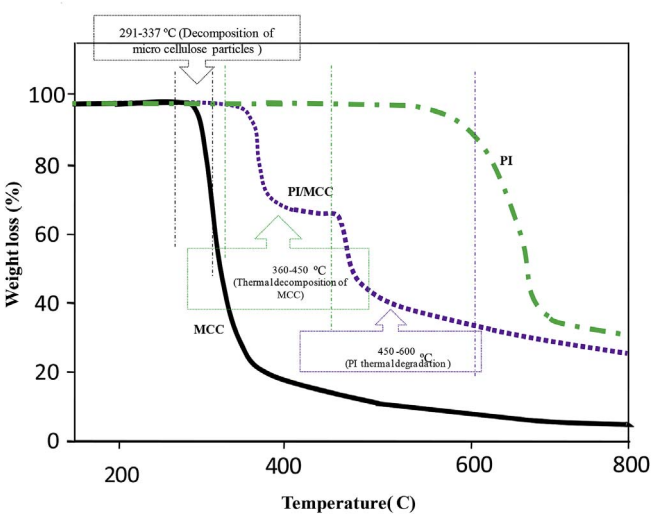


**Fig. 2.** TGA profile for PI, MCC and polymer blends of PI/MCC.

to the PI/NCC, two weight losses were observed in the curve of PI/MCC blending. The first weight loss observed at 360–450 °C that was related to the thermal decomposition of MCC while the second loss from 450 to 600 °C was attributed to the thermal decomposition of PI.

Fig. 3 illustrates the TGA profiles of PVP, PI, and PI/PVP at 9 wt%. PVP started to decompose at 380 °C and completely at 450 °C (Mondal and Mandal, 2014; Salleh and Ismail, 2011). There are two distinct weight losses could be observed in polymer blends of PI/PVP which was the first weight loss observed at 420–480 °C due to the decomposition of PVP while the second weight loss was observed between 480 and 620 °C possibly attributed to the decomposition of PI.

PI had been reported to be a thermosetting polymer (Iredale et al., 2017) while NCC, MCC, and PVP were thermally labile polymer (Lee et al., 2007). Amongst these samples, the blending of the PI/NCC to be the earliest to decompose (in the range between 280 and 375 °C) due to the presence of sulphate groups that forces the blending polymer to decompose at much lower temperature as compared to the others (Mohamed et al., 2015c). Meanwhile, the PI/MCC started to decompose at temperature ranging from 360 to 450 °C and followed by decomposition of PI/PVP at temperature between 420 and 480 °C. The differences of thermal properties of the two polymers showed significant effects on the thermal stability of the final membrane.

### 3.2. Scanning electron microscopy analysis

Fig. 4 shows the micrographs of the PI/NCC precursor and

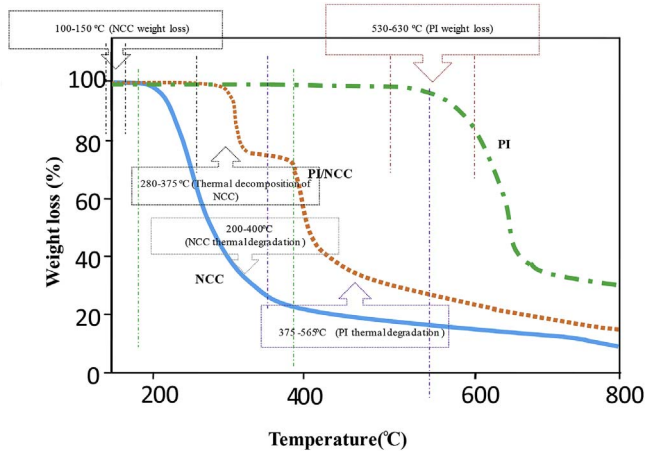


**Fig. 1.** TGA profile for PI, NCC and polymer blends of PI/NCC.

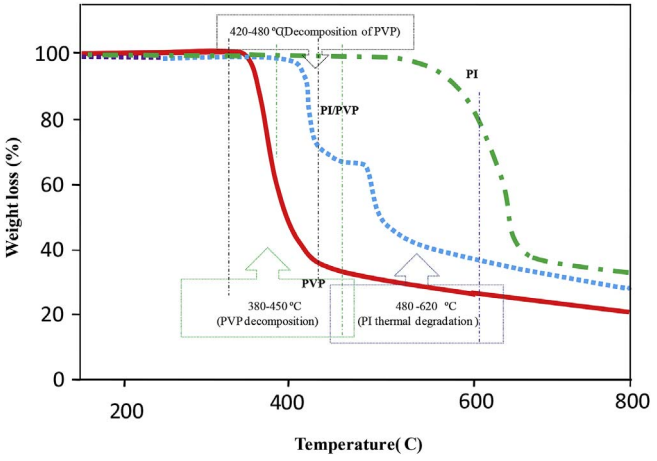


**Fig. 3.** TGA profile for PI, PVP and polymer blends of PI/PVP.

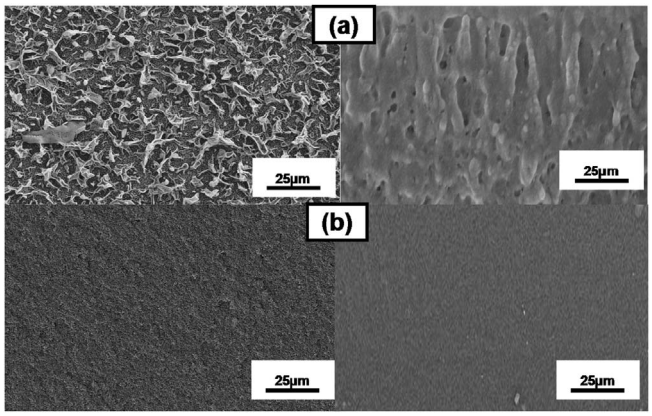


**Fig. 4.** Surface micrographs for **(a)** PI/NCC polymeric membrane, **(b)** PI/NCC-carbon membrane.

carbonized membranes fabricated at different blending compositions. It was observed that the long (needle-shaped), slender rod of NCC particles appeared inside the precursor membrane (Fig. 4 (a)). The morphology was in agreement with the Kaboorani et al. where a rod-like of NCCs with 150–250 nm was observed (Kaboorani et al., 2012). It can be observed that the rods-like NCCs structures were shorter but still contained both microcrystals and aggregated microcrystals. As mentioned by Mohamed et al., who found that the NCC structure was in uniform nanorod or needle-like shapes. The size found to be 5.78 ± 2.14 nm wide and 121.42 ± 32.51 nm long. After undergoing the carbonization process, the rods or needle-like structures were collapsed. These results showed that the PI/NCC membrane with dense structure was obtained.

Fig. 5(a) shows the surface micrograph for PI/MCC polymeric membrane while Fig. 5(b) shows PI/MCC carbon membrane surface micrograph. In order to verify the presence of MCC, surface structure of the corresponding membranes was evaluated. The MCC particles uniformly appeared in the polymer matrix without any preferential orientation. No significant agglomeration was observed. Remarkably, it was noted that the role of hydrolysis reaction on the available MCC polymer could alter the polarity of cellulose. The current finding of morphological properties of cellulose were significantly consistent with previous study by Elsakhawy and Hassan (2007) due to the occurrence of fibers shortening and formation of rod-shaped MCC (Elsakhawy and Hassan, 2007). For heat-treated microcrystalline cellulose with PI, the MCC particles do not appear in the membranes, indicating that all membranes were fully carbonized. Furthermore, there was no influence on the final morphologies of the PI/MCC carbon membrane due to depolymerization that leads to the formation of isolated $sp^2$ carbon

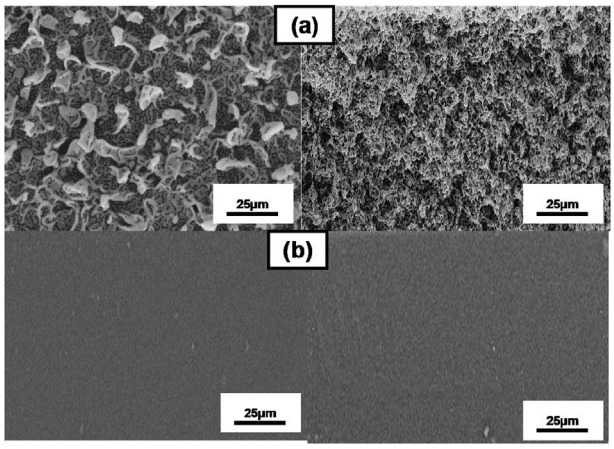


**Fig. 5.** Surface micrographs of **(a)** PI/MCC polymeric membrane and **(b)** PI/MCC- carbon membrane.

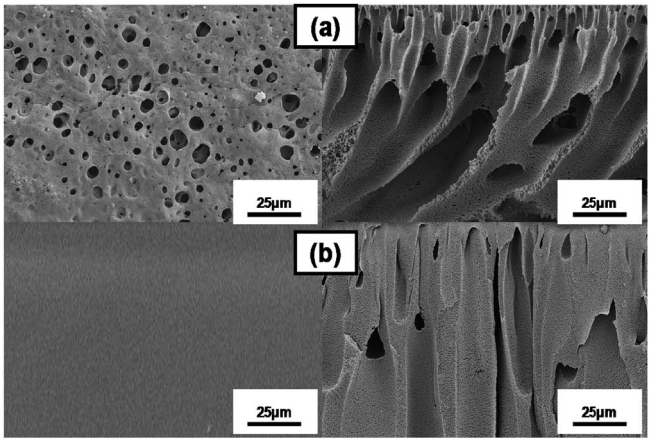


**Fig. 6.** Micrographs of **(a)** PI/PVP polymeric membrane and **(b)** PI/PVP-carbon membrane.

atoms; the same species that is responsible for the increase in overall structure. This effect can be ascribed to the conversion of disordered to ordered $sp^2$ carbon crystallites that increases crystalline thickness, $L_a$ (Hu et al., 2016). In summary, SEM images showed that the addition of different MCC additives inside polymer matrix did not have significant influence to the final carbon structure.

Fig. 6 shows the cross section and outer surface micrographs of PI/PVP precursor and carbonized membranes fabricated at PI/PVP. Based on Fig. 6(a), some closed pores on the outer surface of the membrane were observed that indicated the PI/PVP precursor membrane was filled with microporous structure. This structure was generated because of the rearrangement and movement of the polymer structure. As illustrated in Fig. 6(b), the carbonized membrane showed a reduction in micropores structure which resulted in defect-free and smooth surfaces. The pore distribution was non-homogeneous with wide openings and a few constrictions. This phenomenon signified the occurrence of structural rearrangement of the precursor membrane after the carbonization process (Kim et al., 2005).

### 3.3. Fourier transform infrared spectroscopy (FTIR) analysis

Fig. 7 shows the FTIR spectra of PI/NCC samples. It was observed that the lower peak of 896.73 $cm^{-1}$ was associated with the cellulosic glycosidic linkages that consisted of C1–H and O–H bending (H.P.S et al., 2016). The band at 1052.94 $cm^{-1}$ indicated C–O–C pyranose ring stretching vibration. For PI/NCC carbon membrane, there was a presence of only small peak which indicated the sample was fully converted in carbon form. The hemicellulose characteristic was determined at 1247.71 $cm^{-1}$ that referred to the acyl-oxygen CO-OR stretching vibration in hemicelluloses PI/NCC polymeric membrane (Mohamed et al., 2015c). However, these hemicelluloses could be removed by alkaline treatment. The C=C stretching was observed at peak 1504.20 $cm^{-1}$ where it presented plane symmetrical stretching of the aromatic rings that appeared in lignin of the PI/NCC polymeric membrane. While at peak of 1594.84 $cm^{-1}$, C=C unsaturated linkages presented due to the existence of aromatic rings in lignin for PI/NCC polymeric membrane (Mohamed et al., 2015c).

The FTIR spectra of the PI/MCC samples are shown in Fig. 8. From the figure, band 1120.43 $cm^{-1}$ of PI/MCC polymeric membrane can be clearly seen. This phenomenon indicated –C—O—C—stretch of the β-1,4-glycosidic linkage in cellulose which known as most prominent in MCC. At high wave number of 3000.69–3600.44 $cm^{-1}$, the presence peak in PI/MCC polymeric membrane can be attributed to the –C–O– stretching of the carboxyl and acetyl groups in hemicelluloses (Hu et al., 2016). Furthermore, small peak at 1440.56 $cm^{-1}$ and 1735.62 $cm^{-1}$ appeared in PI/MCC polymeric samples which signified

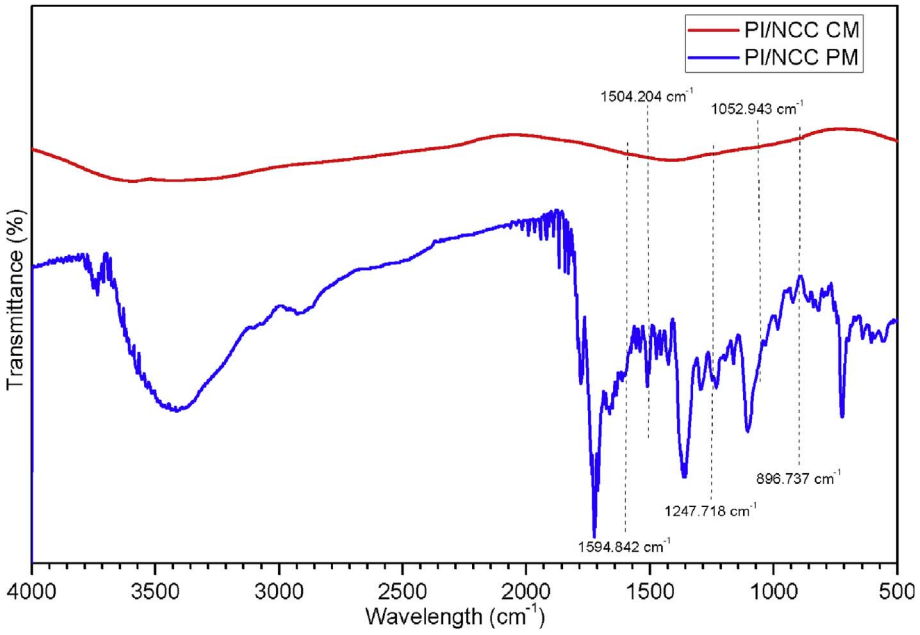


**Fig. 7.** FTIR analysis of PI/NCC-based polymeric and carbon membrane prepared using different dope formulation.

the asymmetric $CH_2$ bending and wagging (Mohamed et al., 2017).

Fig. 9 shows the FTIR spectra of PI/PVP samples. The vibration band at 1650.76 $cm^{-1}$ corresponded to C=O stretching of PVP polymer inside the PI membrane while C-H asymmetric stretching of $CH_2$ absorption band was located at 2987.195 $cm^{-1}$ (Kim et al., 2004). The bands at 931.44 $cm^{-1}$, 1249.64 $cm^{-1}$ and 1427.06 $cm^{-1}$ were attributed to C-C stretching vibration, C-N stretching vibration and C-H bending vibration of PVP blending, respectively. The broad absorption band centered at 3473.16 $cm^{-1}$ was attributed to O-H stretching mode of $H_2O$ absorbed on the surface of the product. The most striking evidence from FTIR spectrum of the PVP stabilized with PI was the broad peak between 1250 and 650 $cm^{-1}$ which corresponded to C-N stretching motion and C=O stretching motion of monomer for PVP, respectively. The narrow absorption peaks centered occurred at 1409.70 $cm^{-1}$ and 2875.34 $cm^{-1}$ in Fig. 9 which was attributed to the C-H bonding due to the presence of PVP. This scenario might be due to the formation of coordinated bond between nitrogen atoms of the PVP.

Based on Figs. 7–9, it can be concluded that PI/NCC, PI/MCC and PI/PVP-based carbon membrane showed reduction in peaks as the samples underwent heat treatment process. This phenomenon was due to the released of the heteroatoms during the carbonization process where it vanished the presence of the functional group in their original state. The elimination of N, O and H elements from the PI/NCC, PI/MCC and PI/PVP resulted in the rearrangement of carbon membrane morphological structure.

### 3.4. Wide-angle x-ray diffraction patterns

The XRD pattern of the polymeric and carbon membrane was illustrated in Fig. 10. The XRD spectra were stacked accordingly in order to show clear x-ray diffraction results without affecting the diffraction angle. XRD was employed to confirm the amorphous nature of the

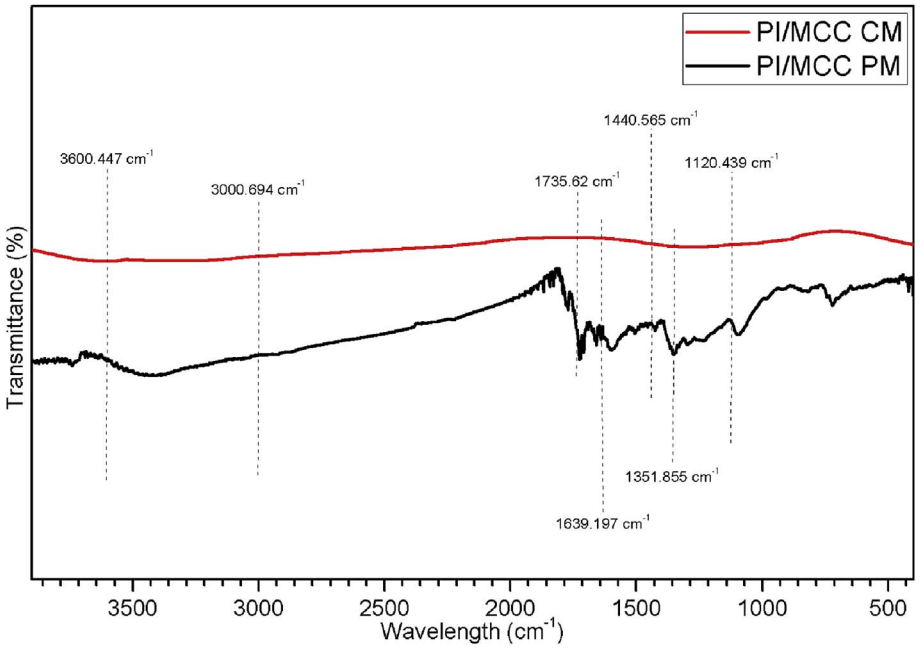


**Fig. 8.** FTIR analysis of PI/MCC-based polymeric and carbon membrane prepared using different dope formulation.

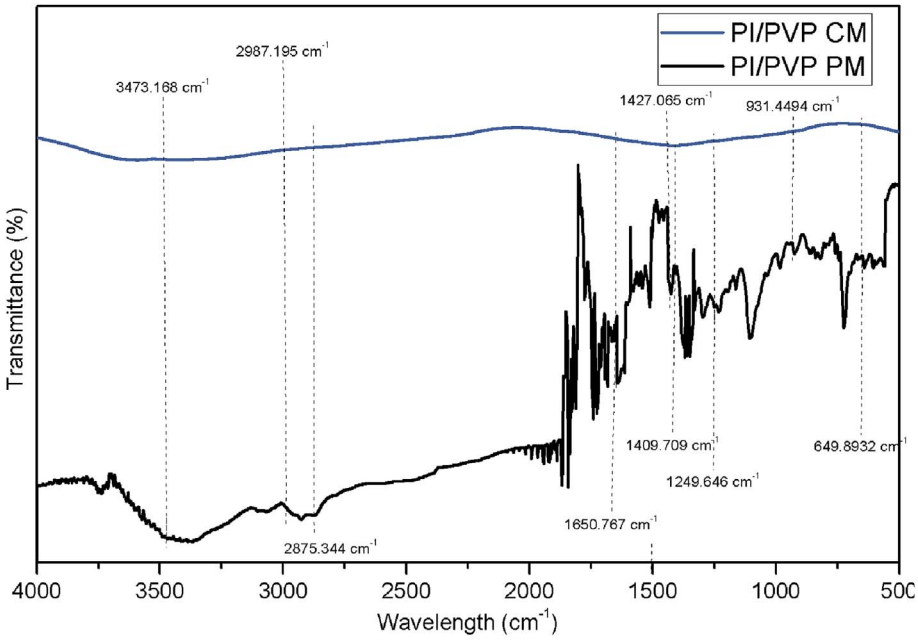


**Fig. 9.** FTIR analysis of PI/PVP-based polymeric and carbon membrane prepared using different dope formulation.

carbon structure. The average *d*-spacing between the individual layers of the carbon were calculated using the Bragg's Law. These *d*-spacing values were determined at the maximum of the broad peaks and only reflected the average space between the centers of the chain segments in the polymer matrix (Wang et al., 2015; Zhang et al., 2014).

The *d*-spacing values of the polymeric membrane prepared from PI/PVP, PI/MCC and PI/NCC were 0.423, 0.417, and 0.403 nm respectively. Whereas, the *d*-spacing values of the carbon membrane prepared from PI/PVP, PI/MCC and PI/NCC were 0.376, 0.369, and 0.356 nm, respectively. It has been suggested that decreases in *d*-spacing value, would results in narrower pore sizes. The small reduction in the average *d*-spacing of the carbon membranes resulted in a very strong molecular sieving effect (Salinas et al., 2017; Briceño et al., 2012). It was revealed that the *d*-spacing value was decreased after the carbonization process. The microstructure of the polymeric was slightly different from that of carbon membranes due to the similar layer distance that could be considered as a divisional path for gas molecules. All samples possessed a broad peak and amorphous structures (Su and Lua, 2007). The

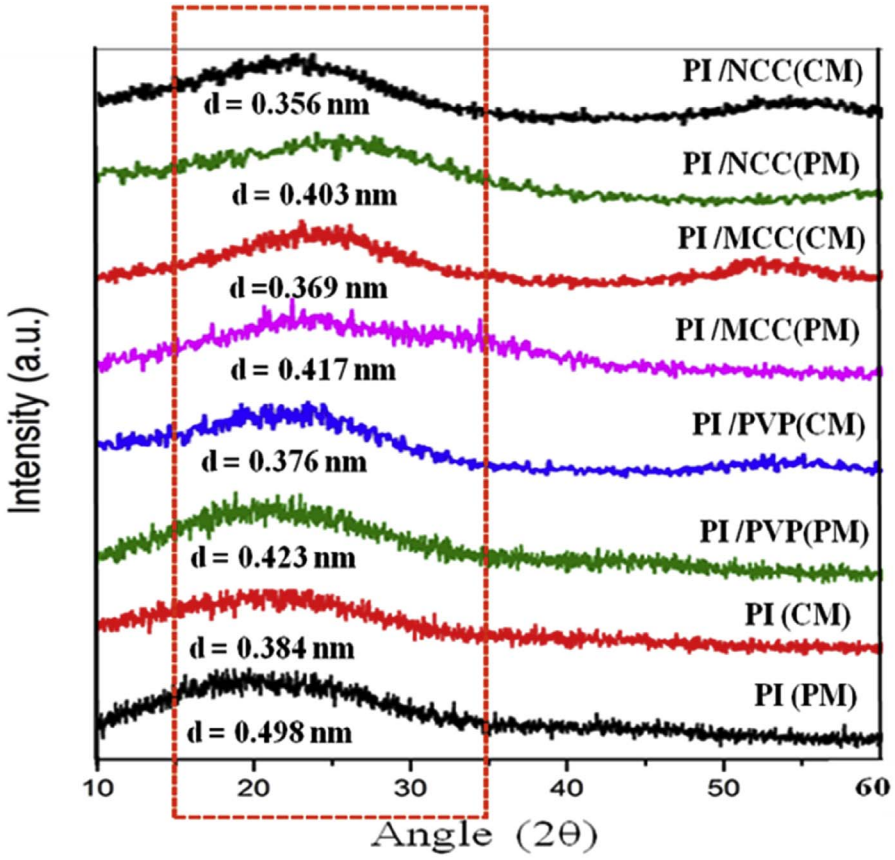


**Fig. 10.** XRD spectra of PI-based polymeric and carbon membrane prepared using different dope formulating.

polymeric and carbon membrane possessed differences in *d*-spacing value which referred to the space dimension for a small gas molecule to penetrate through membrane and it was very helpful information to determine the gas permeability and selectivity.

The carbon membrane from blended PI/NCC provided a low *d*-spacing value of 0.356 nm among other carbon membrane as illustrated in Fig. 10. From the graph, the presented cellulose crystal diffraction pattern peaks were observed at $2\theta = 24.99^{\circ}$ and $2\theta = 22.21^{\circ}$. Moreover, after experiencing different steps of chemical pretreatment using NaOH and $NaClO_2$ and followed by acid hydrolysis process, the crystallinity index of the samples was increased. This phenomenon was due to the lignin removal that occurred during NaOH and $NaClO_2$ pretreatment (Mohamed et al., 2016a). Furthermore, the appearance of a weak diffraction peak could be observed which signified the removal of most of the lignin and hemicelluloses inside the membrane. In addition, the PI/MCC carbon membrane showed decreasing crystallinity degree. This statement might be explained by a reduction of the intra- and intermolecular carbon bonds during the heat treatment process (Shi et al., 2015).

### 3.5. Gas permeation measurements

The gas permeation performances of the polymeric and carbon membrane with different polymer blends are presented in Tables 2 and 3, respectively. From the gas permeation test, it was revealed that the addition of NCC, MCC and PVP to the precursor as an additive produced better gas permeation performance as compared to pure PI. The current finding demonstrated that the highest gas permeance and selectivity was obtained for the PI/NCC polymeric membrane. For all tested membranes, the gas permeance of the selected gases were in the order of $CO_2 > O_2 > CH4 > N_2$.

As tabulated in Table 3, the PI/NCC carbon membrane showed the highest selectivity among the other carbon membranes with resulting values of $CO_2/CH_4$ of 68.23 ± 3.27, $CO_2/N_2$ of 66.32 ± 2.18, and $O_2/N_2$ of 9.29 ± 2.54. As mentioned in the previous studies, the presences of pore performing agent resulted in the formation of porous structure (Siddique et al., 2014; Wu et al., 2016). This scenario was attributed to additives that could be easily decomposed at lower temperature as compared to PI-copolyimide. Consequently, by varying different types of additives might lead to the different pore size, pore volume and diffusional pathway in carbon membranes. Carbon membrane derived from PI/NCC showed a higher gas permeance due to an increased compactness of microporous structures as compared to those prepared from pure PI, PI/MCC and PI/PVP. According to Kim et al., the carbon membrane that prepared with the addition of additives had promoted the enhancement of the diffusion pathway for the gas species in the domain of the thermally liable polymer (Kim et al., 2005).

All selectivity of the gas pair increased dramatically from the polymeric membrane to carbon membrane. The increment of 28, 32 and 6 times was observed for $CO_2/CH_4$, $CO_2/N_2$ and $O_2/N_2$ selectivity, respectively. The carbon membrane derived from PI/PVP showed the lowest gas permeance and selectivity among the PI/NCC and PI/MCC. This phenomenon was mainly due to the difficulties for the small gases molecules to pass through the tiny channels. The permeation results of all the carbon membranes showed that the gas transport was controlled by the molecular sieving mechanism.

It is concluded that the addition of the thermally labile polymer can control the overall pore structure of carbon membranes by fixing carbonization temperatures as well as PI composition. The addition of additives such as cellulose makes the carbon membranes retard the transport of easily condensable gases (e.g. $CO_2$). This phenomenon can be exploited for enhancing gas separation efficiency (Lie and Hägg, 2005). Apart from that, the carbon membrane containing cellulose has demonstrated a promising gas permeation performance for the gas pairs of $O_2/N_2$ and $CO_2/CH_4$ (Lie and Hägg, 2005). In this study, carbon membrane derived from pure PI was less permeable as compared to carbon membrane derived from PI/additives. These results were supported by Kim et al., who reported that the gas permeation results showed that the ideal $O_2/N_2$ separation factor of the membranes was improved by the presence of the additives (Kim et al., 2004). During the heat treatment process, the membrane tended to create cracks due to the presence of additives. In this study, it was believed that the NCC which was carbon content of aromatic structures indicated that the molecules start to stride in their way out and form micropores structure at its thermal degradation temperature same as mention by Xie et al. (Xie et al., 2009). Furthermore, it was proven that the tubular supported carbon membrane derived from PI/NCC membrane has great potential to compete with other available carbon membrane for gas separation application.

## 4. Conclusion

The influence of three types of thermally labile additives on the preparation of the carbon membrane was investigated. The presence of additives (NCC, MCC, and PVP) resulted in decreasing thermal stability of polymer blends. Hence, it might be suggested that the presence of additives can be utilized to fabricate carbon membrane with desirable morphological structure. Moreover, the presence of the additives in carbon membrane provided superior pore structural properties due to the decomposition prior to carbonization process. Among the studied samples, NCC as an additive provided optimum physicochemical properties owing to their nano-crystalline structure. Other than that, the permeances of all gases increased with the addition of additives. The carbon tubular membrane from PI/NCC showed the best composition with $CO_2/CH_4$, $CO_2/N_2$ and $O_2/N_2$ selectivity of 68.23 ± 3.27, 66.32 ± 2.18, and 9.29 ± 2.54, respectively. It was concluded that the utilizing of NCC as thermally labile additive showed positive remarks in carbon membrane development. These findings would be a good initiating point in order to encourage the study of using recycle resources such as NCC as a polymeric additive material.

## Acknowledgements

The authors gratefully acknowledge the financial support from the Malaysian Ministry of Higher Education and Universiti Teknologi Malaysia under Higher Institution Centre of Excellence Scheme (Project

**Table 2**
Gas permeation performance of polymeric membranes.

| Sample | Polymeric membrane | | | | | | |
|---|---|---|---|---|---|---|---|
| | Permeance (GPU) | | | | Selectivity | | |
| | $CH_4$ | $N_2$ | $CO_2$ | $O_2$ | $CO_2/CH_4$ | $CO_2/N_2$ | $O_2/N_2$ |
| PI | 0.68 ± 4.57 | 0.70 ± 5.23 | 1.13 ± 6.32 | 0.77 ± 3.22 | 1.66 ± 3.49 | 1.61 ± 4.21 | 1.10 ± 5.12 |
| PI/NCC | 0.80 ± 2.51 | 0.94 ± 3.54 | 1.92 ± 3.72 | 1.33 ± 2.31 | 2.40 ± 2.19 | 2.04 ± 3.42 | 1.41 ± 1.92 |
| PI/MCC | 0.76 ± 3.29 | 0.80 ± 2.44 | 1.55 ± 1.65 | 1.11 ± 2.19 | 2.04 ± 3.26 | 1.94 ± 6.54 | 1.39 ± 1.09 |
| PI/PVP | 0.78 ± 2.54 | 0.80 ± 3.11 | 1.36 ± 2.43 | 1.09 ± 4.19 | 1.74 ± 3.65 | 1.70 ± 4.98 | 1.37 ± 3.22 |

**Table 3**
Gas permeation performance of carbon membranes.

| Sample | Carbon membrane | | | | | | |
|---|---|---|---|---|---|---|---|
| | Permeance (GPU) | | | | Selectivity | | |
| | $CH_4$ | $N_2$ | $CO_2$ | $O_2$ | $CO_2/CH_4$ | $CO_2/N_2$ | $O_2/N_2$ |
| PI | 2.37 ± 3.32 | 2.78 ± 1.28 | 156.55 ± 2.17 | 20.24 ± 4.51 | 66.05 ± 1.78 | 56.31 ± 4.35 | 7.28 ± 3.82 |
| PI/NCC | 3.13 ± 1.56 | 3.22 ± 3.21 | 213.56 ± 2.17 | 29.90 ± 2.98 | 68.23 ± 3.27 | 66.32 ± 2.18 | 9.29 ± 2.54 |
| PI/MCC | 3.02 ± 3.65 | 3.20 ± 2.65 | 201.37 ± 2.10 | 20.82 ± 4.32 | 66.68 ± 3.29 | 62.93 ± 2.65 | 6.51 ± 4.78 |
| PI/PVP | 2.90 ± 1.25 | 2.99 ± 1.28 | 189.60 ± 4.75 | 16.02 ± 3.29 | 65.38 ± 2.64 | 63.41 ± 1.44 | 5.36 ± 3.21 |

Number: R.J090301.7846.4J188) and Research University Grant Scheme (Project Number: Q.J130000.2546.12H76). The authors would also like to acknowledge technical and management support from Research Management Centre (RMC), Universiti Teknologi Malaysia.

## References


Adewole, J.K., Ahmad, A.L., Ismail, S., Leo, C.P., 2013. Current challenges in membrane separation of CO2 from natural gas: a review. Int. J. Greenh. Gas. Control 17, 46–65.

Bai, H., Wang, X., Zhou, Y., Zhang, L., 2012. Preparation and characterization of poly (vinylidene fluoride) composite membranes blended with nano-crystalline cellulose. Prog. Nat. Sci. Mat. Int. 22, 250–257.

Briceño, K., Montané, D., Garcia-Valls, R., Iulianelli, A., Basile, A., 2012. Fabrication variables affecting the structure and properties of supported carbon molecular sieve membranes for hydrogen separation. J. Memb. Sci. 415–416, 288–297.

Dalane, K., Dai, Z., Mogseth, G., Hillestad, M., Deng, L., 2017. Potential applications of membrane separation for subsea natural gas processing: a review. J. Nat. Gas. Sci. Eng. 39, 101–117.

Das, K., Ray, D., Bandyopadhyay, N.R., Sengupta, S., 2010. Study of the properties of microcrystalline cellulose particles from different renewable resources by XRD, FTIR, nanoindentation, TGA and SEM. J. Polym. Environ. 18, 355–363.

Elsakhawy, M., Hassan, M., 2007. Physical and mechanical properties of microcrystalline cellulose prepared from agricultural residues. Carbohydr. Polym. 67, 1–10.

George, G., Bhoria, N., AlHallaq, S., Abdala, A., Mittal, V., 2016. Polymer membranes for acid gas removal from natural gas. Sep. Purif. Technol 158, 333–356.

H.P.S, A.K., Saurabh, C.K., A.S, A., Nurul Fazita, M.R., Syakir, M.I., Davoudpour, Y., Rafatullah, M., Abdullah, C.K., M. Haafiz, M.K., Dungani, R., 2016. A review on chitosan-cellulose blends and nanocellulose reinforced chitosan biocomposites: properties and their applications. Carbohydr. Polym. 150, 216–226.

Hosseini, S.S., Omidkhah, M.R., Zarringhalam Moghaddam, A., Pirouzfar, V., Krantz, W.B., Tan, N.R., 2014. Enhancing the properties and gas permeation performance of PBI–polyimides blend carbon molecular sieve membranes via optimization of the pyrolysis process. Sep. Purif. Technol. 122, 278–289.

Hu, L., Li, Z., Wu, Z., Lin, L., Zhou, S., 2016. Catalytic hydrolysis of microcrystalline and rice straw-derived cellulose over a chlorine-doped magnetic carbonaceous solid acid. Ind. Crops Prod. 84, 408–417.

Hunt, A.J., Sin, E.H.K., Marriott, R., Clark, J.H., 2010. Generation, capture, and utilization of industrial carbon dioxide. ChemSusChem 3, 306–322.

Iredale, R.J., Ward, C., Hamerton, I., 2017. Modern advances in bismaleimide resin technology: a 21st century perspective on the chemistry of addition polyimides. Prog. Polym. Sci. 69, 1–21.

Itta, A.K., Tseng, H.-H., Wey, M.-Y., 2011. Fabrication and characterization of PPO/PVP blend carbon molecular sieve membranes for $H_2/N_2$ and $H_2/CH_4$ separation. J. Memb. Sci. 372, 387–395.

Jones, C.W., Koros, W.J., 1994. Carbon molecular sieve gas separation membranes-I. Preparation and characterization based on polyimide precursors. Carbon N. Y. 32, 1419–1425.

Kaboorani, A., Riedl, B., Blanchet, P., Fellin, M., Hosseinaei, O., Wang, S., 2012. Nanocrystalline cellulose (NCC): a renewable nano-material for polyvinyl acetate (PVA) adhesive. Eur. Polym. J. 48, 1829–1837.

Kim, Y., Park, H., Lee, Y., 2005. Gas separation properties of carbon molecular sieve membranes derived from polyimide/polyvinylpyrrolidone blends: effect of the molecular weight of polyvinylpyrrolidone. J. Memb. Sci. 251, 159–167.

Kim, Y.K., Park, H.B., Lee, Y.M., 2004. Carbon molecular sieve membranes derived from thermally labile polymer containing blend polymers and their gas separation properties. J. Memb. Sci. 243, 9–17.

Koresh, J.E., Soffer, A., 1986. Mechanism of permeation through molecular-sieve carbon membrane. Part 1. The effect of adsorption and the dependence on pressure. J. Chem. Soc. Faraday Trans. 1 Phys. Chem. Condens. Phases 82, 2057.

Lee, H., Suda, H., Haraya, K., 2007. Preparation of carbon membranes derived from polymer blends in the presence of a thermally labile polymer. Sep. Sci. Technol. 42, 59–71.

Lie, J.A., Hägg, M.-B., 2005. Carbon membranes from cellulose and metal loaded cellulose. Carbon N. Y. 43, 2600–2607.

Mohamed, M.A., Abd Mutalib, M., Mohd Hir, Z.A., M. Zain, M.F., Mohamad, A.B., Jeffery Minggu, L., Awang, N.A., Salleh, W.N.W., 2017a. An overview on cellulose-based material in tailoring bio-hybrid nanostructured photocatalysts for water treatment and renewable energy applications. Int. J. Biol. Macromol. 103, 1232–1256.

Mohamed, M.A., Jaafar, J., Ismail, A.F., Rahman, M.A., 2017. Fourier Transform infrared (FTIR) spectroscopy. In: Nidal, H., Ahmad Fauzi, I., Takeshi, M., Darren, O.-R. (Eds.), Membrane Characterization. Elsevier, pp. 3–29.

Mohamed, M.A., Salleh, W.N.W., Jaafar, J., Ismail, A.F., Abd Mutalib, M., Jamil, S.M., 2015a. Incorporation of N-doped TiO2 nanorods in regenerated cellulose thin films fabricated from recycled newspaper as a green portable photocatalyst. Carbohydr. Polym. 133, 429–437.

Mohamed, M.A., Salleh, W.N.W., Jaafar, J., Ismail, A.F., Abd Mutalib, M., Jamil, S.M., 2015b. Feasibility of recycled newspaper as cellulose source for regenerated cellulose membrane fabrication. J. Appl. Polym. Sci. 132 n/a-n/a).

Mohamed, M.A., Salleh, W.N.W., Jaafar, J., Ismail, A.F., Abd Mutalib, M., Mohamad, A.B., M. Zain, M.F., Awang, N.A., Mohd Hir, Z.A., 2017b. Physicochemical characterization of cellulose nanocrystal and nanoporous self-assembled CNC membrane derived from Ceiba pentandra. Carbohydr. Polym. 157, 1892–1902.

Mohamed, M.A., Salleh, W.N.W., Jaafar, J., Ismail, A.F., Mutalib, M.A., Sani, N.A.A., Asri, S.E.A.M., Ong, C.S., 2016a. Physicochemical characteristic of regenerated cellulose/N-doped TiO2 nanocomposite membrane fabricated from recycled newspaper with photocatalytic activity under UV and visible light irradiation. Chem. Eng. J. 284, 202–215.

Mohamed, M.A., Salleh, W.N.W., Jaafar, J., Asri, S.E.A.M., Ismail, A.F., 2015c. Physicochemical properties of "green" nanocrystalline cellulose isolated from recycled newspaper. RSC Adv. 5, 29842–29849.

Mohamed, M.A., Salleh, W.N.W., Jaafar, J., Mohd Hir, Z.A., Rosmi, M.S., Abd Mutalib, M., Ismail, A.F., Tanemura, M., 2016b. Regenerated cellulose membrane as bio-template for in-situ growth of visible-light driven C-modified mesoporous titania. Carbohydr. Polym. 146, 166–173.

Mohamed, M.A., Salleh, W.N.W., Jaafar, J., Rosmi, M.S., Mohd Hir, Z.A., Abd Mutalib, M., Ismail, A.F., Tanemura, M., 2017c. Carbon as amorphous shell and interstitial dopant in mesoporous rutile TiO2: bio-template assisted sol-gel synthesis and photocatalytic activity. Appl. Surf. Sci. 393, 46–59.

Mondal, A., Mandal, B., 2014. CO2 separation using thermally stable crosslinked poly (vinyl alcohol) membrane blended with polyvinylpyrrolidone/polyethyleneimine/tetraethylenepentamine. J. Memb. Sci. 460, 126–138.

Pirouzfar, V., Moghaddam, A.Z., Omidkhah, M.R., Hosseini, S.S., 2014. Investigating the effect of dianhydride type and pyrolysis condition on the gas permeation performance of membranes derived from blended polyimides through statistical analysis. J. Ind. Eng. Chem. 20, 1061–1070.

Rhim, Y.-R., Zhang, D., Rooney, M., Nagle, D.C., Fairbrother, D.H., Herman, C., Drewry, D.G., 2010. Changes in the thermophysical properties of microcrystalline cellulose as function of carbonization temperature. Carbon N. Y. 48, 31–40.

Rubentheren, V., Ward, T.A., Chee, C.Y., Nair, P., Salami, E., Fearday, C., 2016. Effects of heat treatment on chitosan nanocomposite film reinforced with nanocrystalline cellulose and tannic acid. Carbohydr. Polym. 140, 202–208.

Rungta, M., Xu, L., Koros, W.J., 2015. Structure–performance characterization for carbon molecular sieve membranes using molecular scale gas probes. Carbon N. Y. 85, 429–442.

Salleh, W.N.W., Ismail, A.F., 2011. Carbon hollow fiber membranes derived from PEI/PVP for gas separation. Sep. Purif. Technol. 80, 541–548.

Salinas, O., Ma, X., Wang, Y., Han, Y., Pinnau, I., 2017. Carbon molecular sieve membrane from a microporous spirobisindane-based polyimide precursor with enhanced ethylene/ethane mixed-gas selectivity. Rsc. Adv. 7, 3265–3272.

Sazali, N., Salleh, W.N.W., Ismail, A.F., 2017. Carbon tubular membranes from nanocrystalline cellulose blended with P84 co-polyimide for $H_2$ and He separation. Int. J. Hydrogen Energy 42, 9952–9957.

Sazali, N., Salleh, W.N.W., Md Nordin, N.A.H., Harun, Z., Ismail, A.F., 2015a. Matrimid-based carbon tubular membranes: the effect of the polymer composition. J. Appl. Polym. Sci. 132 n/a-n/a).

Sazali, N., Salleh, W.N.W., Md Nordin, N.A.H., Ismail, A.F., 2015b. Matrimid-based carbon tubular membrane: effect of carbonization environment. J. Ind. Eng. Chem. 32, 167–171.

Shi, S.Q., Che, W., Liang, K., Xia, C., Zhang, D., 2015. Phase transitions of carbon-encapsulated iron oxide nanoparticles during the carbonization of cellulose at various pyrolysis temperatures. J. Anal. Appl. Pyrolysis 115, 1–6.

Siddique, H., Bhole, Y., Peeva, L.G., Livingston, A.G., 2014. Pore preserving crosslinkers for polyimide OSN membranes. J. Memb. Sci. 465, 138–150.

Su, J., Lua, A.C., 2007. Effects of carbonisation atmosphere on the structural characteristics and transport properties of carbon membranes prepared from Kapton® polyimide. J. Memb. Sci. 305, 263–270.

Sun, Y., Liu, P., Liu, Z., 2016. Catalytic conversion of carbohydrates to 5-

hydroxymethylfurfural from the waste liquid of acid hydrolysis NCC. Carbohydr. Polym. 142, 177–182.
Tanihara, N., Shimazaki, H., Hirayama, Y., Nakanishi, S., Yoshinaga, T., Kusuki, Y., 1999. Gas permeation properties of asymmetric carbon hollow fiber membranes prepared from asymmetric polyimide hollow fiber. J. Memb. Sci. 160, 179–186.
Tiptipakorn, S., Damrongsakkul, S., Ando, S., Hemvichian, K., Rimdusit, S., 2007. Thermal degradation behaviors of polybenzoxazine and silicon-containing polyimide blends. Polym. Degrad. Stab. 92, 1265–1278.
Wang, S., Tian, Z., Feng, J., Wu, H., Li, Y., Liu, Y., Li, X., Xin, Q., Jiang, Z., 2015. Enhanced CO2 separation properties by incorporating poly(ethylene glycol)-containing polymeric submicrospheres into polyimide membrane. J. Memb. Sci. 473, 310–317.
Wu, C.-Y., Hu, C.-C., Lin, L.-K., Lai, J.-Y., Liu, Y.-L., 2016. Liberation of small molecules in polyimide membrane formation: an effect on gas separation properties. J. Memb. Sci. 499, 20–27.
Xie, X., Goodell, B., Zhang, D., Nagle, D.C., Qian, Y., Peterson, M.L., Jellison, J., 2009. Characterization of carbons derived from cellulose and lignin and their oxidative behavior. Bioresour. Technol. 100, 1797–1802.
Xing, D.Y., Chan, S.Y., Chung, T.-S., 2013. Fabrication of porous and interconnected PBI/P84 ultrafiltration membranes using [EMIM]OAc as the green solvent. Chem. Eng. Sci. 87, 194–203.
Yong, W.F., Lee, Z.K., Chung, T.-S., Weber, M., Staudt, C., Maletzko, C., 2016. Blends of a polymer of intrinsic microporosity and partially sulfonated polyphenylenesulfone for gas separation. ChemSusChem 9, 1953–1962.
Zhang, M.Y., Niu, H.Q., Qi, S.L., Tian, G.F., Wang, X.D., Wu, D.Z., 2014. Structure evolutions involved in the carbonization of polyimide fibers with different chemical constitution. Mat. Today Commun. 1, 1–8.